Water Air Soil Pollut (2015) 226:2212
DOI 10.1007/s11270-014-2212-6

Adsorption of Cobalt(II) from Aqueous Solutions by Fe_3O_4/Bentonite Nanocomposite

Saeedeh Hashemian · Hossein Saffari · Saeedeh Ragabion

Received: 7 January 2014 / Accepted: 4 November 2014

Abstract Fe_3O_4 and Fe_3O_4/bentonite were prepared by chemical co-precipitation method. They were characterized by X-ray powder diffraction (XRD), Fourier infrared spectroscopy (FTIR), and transmission electron microscope (TEM). Adsorption of cobalt(II) on the bentonite, Fe_3O_4, and Fe_3O_4/bentonite nanocomposite was studied. The results indicated that the metal oxides mainly occurred in the form of spinel structure of Fe_3O_4 and the presence of Fe_3O_4 significantly affect the surface area and pore structure of the bentonite. The specific surface area (Brunauer–Emmett–Teller (BET) method) of bentonite, Fe_3O_4, and Fe_3O_4/bentonite were determined to be 34.44, 98.44, and 140.5 $m^2\ g^{-1}$, respectively. TEM image of Fe_3O_4/bentonite shows the particle diameter at 10 nm. The maximum adsorption capacity of cobalt(II) by Fe_3O_4/bentonite nanocomposite was determined to be 18.76 mg g^{-1}. The adsorption strongly depends on pH, where the removal efficiency increases as the pH turns to alkaline range (pH 9). The results suggest that higher adsorption capacity of composite than bentonite is attributed to the presence of Fe_3O_4. The adsorption process follows pseudo-second-order kinetics. The equilibrium data was analyzed by Langmuir model showing high correlation coefficient. The thermodynamic study of adsorption process showed that the adsorption of Co(II) onto Fe_3O_4 /bentonite was carried out spontaneously.

S. Hashemian (✉) · H. Saffari · S. Ragabion
Chemistry Department, Islamic Azad University, Yazd, Iran
e-mail: Sa_hashemian@iauyazd.ac.ir

Keywords Adsorption · Bentonite · Co(II) · Fe_3O_4 / bentonite · Nanocomposite

1 Introduction

One of the major problems concerning industrial wastewaters is heavy metals effluent. The presence of toxic metals in aqueous systems has become a problem due to their harmful effects on human health and other organisms in the environment (Ramakrishna and Viraraghavan 1997). Heavy metals are considered to be nonbiodegradable. These metals are introduced into natural water resources by wastewater discharged from industries such as smelting, metal playing, cosmetic, stabilizer, and alloy manufacturing (Gallions and Vaclavikova 2008; Naiya et al. 2009). Adsorption has gained favor in recent years due to proven efficiency in the removal of pollutants from effluents to stable forms (Gupta et al. 2003; Hashemian 2010). Therefore, adsorption process is one of the effective methods with the advantages of high treatment efficiency and no harmful by-product to treat water (Eren and Afsin 2008; Hashemian and Foroghimoqhadam 2014). Natural clays are low cost and readily available materials functioning as excellent cation exchangers. The adsorption capacity of clays is resulted from a relatively high surface area and a net negative charge on their structure, which attracts and holds cations such as heavy metals (Hashemian 2007; Namasivayam and Sureshkumar 2008; Khenifi et al. 2007; Oliveira et al. 2003).

The application of magnetic particles technology to solve environmental problem is also considered.

Published online: 07 December 2014

Magnetic particles can be used to adsorb contaminants from aqueous or gaseous effluents after the adsorption is carried out. The magnetic adsorbent can be separated from the medium by a simple magnetic process. Therefore, there has been a growing interest in inexpensive high surface area materials, especially metal oxides, due to their unique application, including adsorption and chemical catalysis (Wu and Qu 2005). Most of these materials have the drawbacks of small adsorption capacity and narrow application range. For example, $MnFe_2O_4$ powder and $MnO–Fe_2O_3$ composite could only be used to adsorb ionic organic pollutants. In addition, the applicable pH range of these materials was relatively narrow (Wu et al. 2005). To overcome the disadvantages of sorbents and magnetic particles, several methods such as impregnation, ball milling, and chemical co-precipitation, have been developed to combine them with each other to produce magnetic composite, which could be used as adsorbents to remove a wide range of organic pollutants. Among these methods, chemical co-precipitation is the most promising method, because it is simple and no special chemicals and procedures are needed (Hashemian 2010, 2011; Wu et al. 2004; Zhang et al. 2007; Yang 2008).

Bentonite was used for adsorption of radioactive wastes and their sorption properties were investigated (Galamboš et al. 2011, 2012; Mockovčiaková et al. 2010). The magnetic clays and bentonites were also investigated for adsorption of cadmium(II) and nickel from aqueous solution (Vereš et al. 2010; Orolínová et al. 2010). The removal of Co(II) from aqueous solutions was studied by adsorption on natural clinoptilolite (Smiciklas et al. 2007), kaolinite (Yavuz et al. 2003), chitosan-coated perlite(Kalyani et al. 2007), activated carbon prepared from apricot stone (Kobya et al. 2005), and sepiolite(Kara et al. 2003).

The aim of this research was to investigate the capability of bentonite, Fe_3O_4, and Fe_3O_4/bentonite composite as sorbents for removal of Co^{2+} from aqueous solution.

2 Experimental

2.1 Chemical and Materials

Ferro(II) chloride dihydrate, ferric chloride, and Co(II) nitrate were obtained from Merck. All other chemicals and reagents were in analytical grade and used without any purification.

2.2 Preparation of Fe_3O_4

Fe_3O_4 was prepared by using chemical co-precipitation method; 2 mmol of Fe(II) chloride and 4 mmol Fe(III) chloride were dissolved in the distilled water; then under vigorous magnetic stirring at 70 °C, NaOH solution (5 %) was added drop wise to raise the suspension pH to about 10 and the stirring continued for 1 h. After being cooled, the prepared Fe_3O_4 was repeatedly washed with distilled water and dried in an oven at 105 °C for 2 h.

2.3 Preparation of Fe_3O_4/Bentonite Magnetic Composite

Fe_3O_4/bentonite magnetic composite was prepared by using a co-precipitation method. The bentonite was added into a 400-mL solution containing ferro(II) chloride (0.02 mol) and ferric chloride (0.04 mol) at room temperature. The amount of bentonite was adjusted to obtain Fe_3O_4/bentonite mass ratio of 1:10 under vigorous magnetic stirring, the pH was slowly raised by adding NaOH (5 %) solution to about 10 and stirring continued for 30 min, and stirring was then stopped. The suspension was heated to 95–110 °C for 2 h. After cooling, the prepared magnetic composite was repeatedly washed with distilled water. Through a simple magnetic procedure, the obtained materials were separated from water and dried in an oven at 110 °C.

2.4 Adsorption Studies

In order to study the effect of different parameters such as the contact time, pH, and sorbent dosage on the sorption, various experiments have been carried out by agitation of known amount of sorbents (0.1 g) in 50 mL of Co(II) solution with an initial concentration of 800 mg L^{-1} on rotary shaker at a constant speed of 150 rpm at room temperature (25 °C). The effect of pH was studied by adjusting the pH of solutions in the range of 2–9 with 0.1 N NaOH or HCl solutions. To evaluate the adsorption thermodynamic parameters, the effect of temperature on adsorption were carried out at 15–60 °C. Each experiment was repeated five times, and the average results were given. Relative standard

deviation (% RSD) was determined between 1.8 and 3.1 % for each points at all the experiments.

The percent removal of Co by the hereby adsorbent is given by:

$$\%\,\text{Removal} = (C_0 - C_e)/C_0 \times 100$$

Where C_0 and C_e refer to the initial and equilibrium concentrations (mg L^{-1}) of Co, respectively.

2.5 Methods

Infrared spectrum is recorded using Fourier infrared spectroscopy (FTIR) instrument (Bruker, Tensor T27) for all samples in KBr medium between the 400 and 4000 cm^{-1}. The crystalline structure of Fe_3O_4 in the composite was determined via the X-ray powder diffraction (XRD) method using an Endeavor D4 with Cu Kα radiation. pH measurement was done by a Horiba pH meter (M13, Japan). A transmission electron microscope (TEM) Philips CM200 was used to characterize the Fe_3O_4/bentonite composite with respect to their particle size and shape. The surface area of the samples was determined using Brunauer–Emmett–Teller (BET) Quantachrome Autosorb-1 analyzer. Elemental analysis by atomic absorption spectrophotometry (AAS) was performed on a Shimadzu AA-6800. From the results of elemental analysis, percentage of Fe form Fe_3O_4 was determined to be 8.7 %.

3 Results and Discussion

3.1 Characterization of Adsorbents

The composites were prepared by the precipitation of Fe_3O_4 onto bentonite surface. The magnetism test with a permanent magnet (2300 G) showed that the material was magnetic and completely attracted to the magnet.

The chemical composition of bentonite from XRF is shown in Table 1. Table 1 indicates the presence of silica and alumina as major constituents along with traces of sodium, potassium, iron, magnesium, and calcium oxides in the form of impurities.

Figure 1a–c shows the XRD diffraction patterns for bentonite, Fe_3O_4, Fe_3O_4/bentonite nanoparticles, respectively. XRD indicated the presence of free quartz in bentonite (2θ=27° and d=3.34 Å). It is, thus, expected that the adsorbate species will be removed mainly by

Table 1 Chemical composition of bentonite

Component	Weight (%)
SiO_2	63.91
Al_2O_3	13.8
MgO	3.52
Fe_2O_3	2.67
CaO	1.21
Na_2O	1.79
K_2O	2.11
LOI	11.37
SO_3	0.07

SiO_2 and Al_2O_3 (Fig. 1a). The XRD analysis of Fe_3O_4 (Fig. 1b) indicated that the metal oxides mainly occurred in the form of spinel structure of Fe_3O_4. From the XRD pattern of Fe_3O_4, the characteristic peaks of Fe_3O_4 were observed at 2θ=30.2°, 33.5°, 37, 43.1°, 57°, and 63°. It showed that Fe_3O_4 is the main phase in both samples of Fe_3O_4 and Fe_3O_4/bentonite (Chang and Chen 2005). Fe_3O_4 had cubic unite cell ($a=b=c$=8.33°A and $\alpha=\beta=\gamma$=90°) with FCC system. The X-ray diffraction patterns showed well-developed diffraction lines assigned to pure spinel phase, with all major peaks matching the standard pattern of Fe_3O_4, JCPDS 8-0234. From results of XRD, the binding process of bentonite did not result in the phase change of Fe_3O_4.

The average crystallite size of the sorbents has been estimated through the broadening of the X-ray diffraction peak using the Scherrer's equation (Özer et al. 2007) at about 63, 45, and 12 nm for bentonite, Fe_3O_4, and Fe_3O_4/bentonite composite, respectively (Villalba et al. 2010).

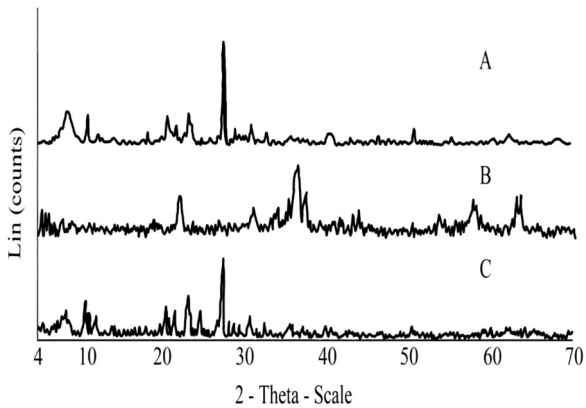

Fig. 1 Powder XRD patterns for the *A* bentonite, *B* Fe_3O_4, and *C* Fe_3O_4/bentonite composite

Figure 2 shows FTIR spectra of (a) bentonite, (b) Fe_3O_4, and (c) Fe_3O_4/bentonite composite. FTIR spectrum of bentonite, the peaks at 3632 and 3426 cm^{-1} are O–H stretching and H–O–H hydrogen-binding water. The peak of 1638 cm^{-1} is H–O–H deformation. The peak of 1021 cm^{-1} is Si–O–Si, the sharp peak of 783 cm^{-1} is due to Si–O stretching of quartz and silica, peak of 514 cm^{-1} is related to Al–O–Si deformation, and the peak of 467 cm^{-1} is related to Si–O–Si deformation. In the FTIR of Fe_3O_4, the peak at 581 cm^{-1} is related to Fe–O group. The results from FTIR analyses (Fig. 2) revealed the formation of two asymmetric bands between 467 and 785 cm^{-1}, typical of the spinel structure of Fe_3O_4 (Meng et al. 2005).

The typical TEM micrograph of the Fe_3O_4/bentonite nanoparticles is shown in Fig. 3. It is clear the nanoparticles had a mean diameter of 10 nm, substantially consistent with the results estimated from Scherrer's formula. The composite had a uniformed distribution of spherical particles. This reveals that the binding process did not significantly result in the agglomeration. This could be attributed to the reaction occurring only on the particle surface.

3.2 Effect of Contact Time on Adsorption of Co(II)

The effect of contact time of adsorption of cobalt(II) onto bentonite, Fe_3O_4, and Fe_3O_4/bentonite composite is shown in Fig. 4. For bentonite and Fe_3O_4 magnetic ferrite adsorption efficiency is about 56 and 77 % after 90 min contact time, respectively, but for Fe_3O_4/bentonite composite adsorption efficiency can be close to 97 %, after 10 min contact time, which shows Fe_3O_4/bentonite composite, exhibits an excellent adsorbent/catalyst. Similar results were obtained for azo dye acid red B and acid orange (Zhang et al. 2007; Wu et al. 2005). The adsorption process could be divided into two steps, a quick step and a slow one. In the first step, the adsorption rate was fast, and 97 % of the equilibrium adsorption capacity was achieved within 10 min. In the subsequent step, the adsorption was slow and reached equilibrium at 1 h. It is obvious from the fact that a large number of surface sites are available for adsorption at the initial stages, and after a lapse of time, the remaining surface sites are difficult to be occupied because of the repulsion between the solute molecules of the solid and the bulk phase occurred. This is due to higher contact between the sorbent surface and Co ions.

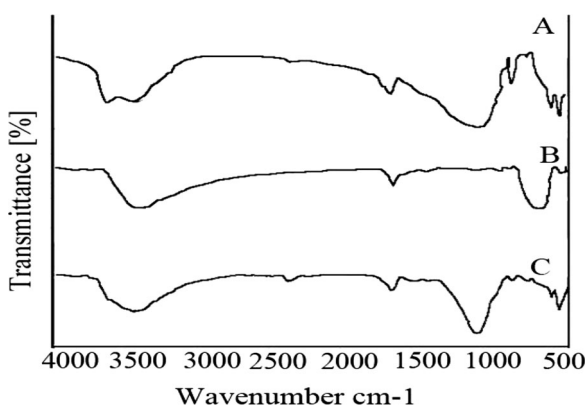

Fig. 2 FTIR spectra of *A* bentonite, *B* Fe_3O_4, and *C* Fe_3O_4/bentonite composite

The specific surface area (BET method) of bentonite, Fe_3O_4, and Fe_3O_4/bentonite composite were 34.44, 98.44, and 140.5 $m^2\ g^{-1}$, respectively. Presence of Fe_3O_4 on the bentonite increased the surface area of composite, therefore the contact time of Co(II) with Fe_3O_4/bentonite composite was decreased.

3.3 Effect of pH

The effect of pH on the adsorption of Co(II) onto Fe_3O_4/bentonite was studied by varying the pH of solution from 2 to 9. The experiments were carried out for 50 mL of Co(II) with initial concentration of 500 and 800 mg L^{-1} and 0.1 g of sorbents for 15 min contact time. It is evident that the amount of adsorption strongly depends on pH solution of media. The adsorption percentage of Co(II) by Fe_3O_4/bentonite is increased with the increase of the pH value, and the maximum uptake of the Co(II) takes place at around pH 8 (Fig. 5). It was noticed that when the pH value was higher than 5, the adsorption amount increased dramatically; this was attributed to the fact that heavy metal ions started to precipitate, leading to the reduction of the metal ions in the aqueous solution at higher pH value. Therefore, when pH value is greater than 5, the adsorption amount increases little by little (Feng et al. 2010).

The adsorption of Co(II) decreases with decreasing pH because the aluminol and silanol groups are more protonated and, hence, they are less available to retain the investigated metals. The reason of this behavior is that the surface complexation reactions are also influenced by the electrostatic attraction between the surface charge and the dissolved ions (Abollino et al. 2003). The

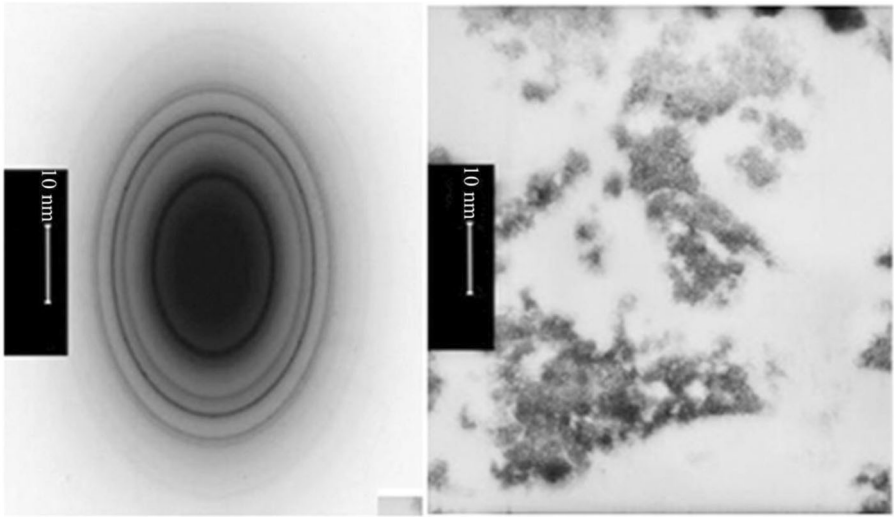

Fig. 3 TEM image of Fe_3O_4/bentonite nanocomposite

results of cobalt analysis showed that up to pH values around 8, the dominant chemical form of Co in the aqueous media was Co(II). Beyond pH 9.0, CoOH+ and Co $(OH)_2$(aq) became increasingly prominent (Üzüm et al. 2009). It is outstanding; bentonite is a clay mineral with ion exchange properties. Therefore, for each Co(II) adsorbed, an equivalent amount of Na ion is released from the bentonite surface. Metal removal by adsorption onto Fe_3O_4/bentonite is much more efficient compared with metal hydroxide precipitation (Rengaraj et al. 2002). Hydroxy complexes of Co(II) ions such as $CoOH^+$ formed at pH >8.2 leads to an increase in the number of positive charges on Fe_3O_4/bentonite. Adsorption of such ions onto Fe_3O_4/bentonite through electrostatic attraction can impart Fe_3O_4/bentonite more positive charges.

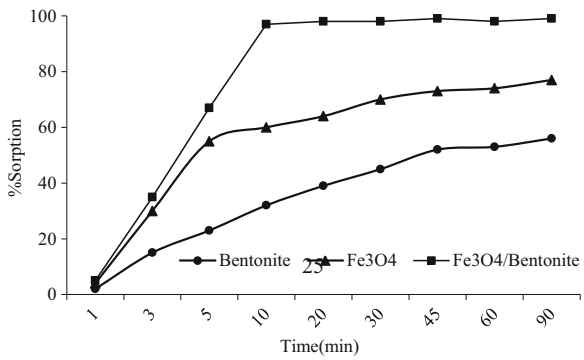

Fig. 4 Effect of contact time of adsorption Co(II) onto bentonite, Fe_3O_4, and Fe_3O_4/bentonite composite (50 mL of Co(II) 800 mg L^{-1})

3.4 Effect of Amount of Sorbent

The results of the effect of composite dose on experiments carried out using 50 mL of Co(II) with initial concentration 500 and 800 mg L^{-1} and pH 10. The results are shown in Fig. 6. Removal efficiency for Co increased up to 99 % at 0.1 g Fe_3O_4/bentonite and then, remained constant regardless of the increase in the adsorbent dose. The positive correlation between adsorbent dose and removal efficiency is related to increasing surface area of available exchangeable sites (Hashemian 2011).

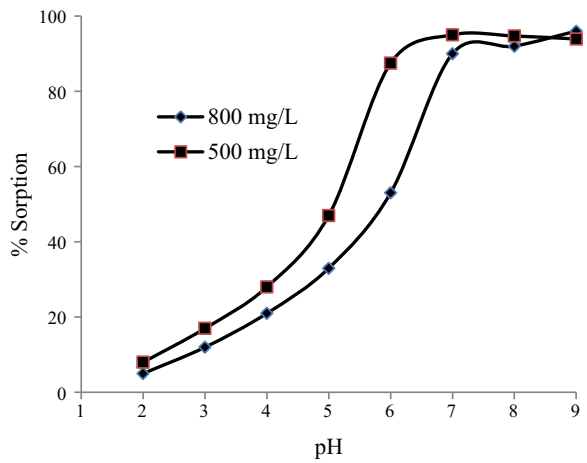

Fig. 5 Effect of pH on adsorption of Co(II) onto bentonite, Fe_3O_4, and Fe_3O_4/bentonite composite (50 mL of Co(II) 500 and 800 mg L^{-1}, 0.1 g sorbent)

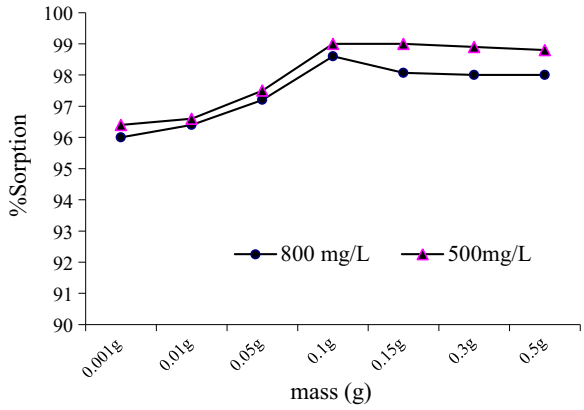

Fig. 6 Effect of amount of Fe_3O_4/bentonite composite on the sorption of Co(II) (50 mL of Co(II) solution, initial concentrations 500, and 800 mg L^{-1}, pH 8)

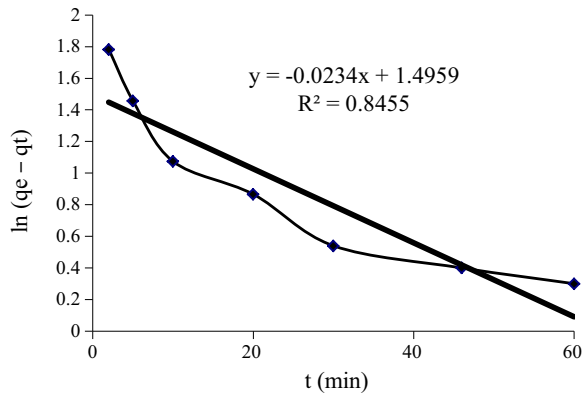

Fig. 7 Pseudo-first-order kinetics for adsorption of Co(II) on Fe_3O_4/bentonite composite (50 mL Co(II) solution, initial concentration 800 mg L^{-1}, pH 8, and 0.1 g sorbent)

3.5 Kinetic of Adsorption

In order to predict adsorption kinetic model of cobalt solutions, pseudo-first-order and pseudo-second-order kinetic models were applied to the data. The pseudo-first-order model assumes that the rate of change of solute uptake with time is directly proportional to difference in saturation concentration and amount of solid uptake with time (Tamez Uddin et al. 2009; Akcay 2004).

$$\ln(q_e - q_t) = \ln q_e - k_1 t \quad (1)$$

Where q_e and q_t are the amounts of Co(II) adsorbed per unit mass of the adsorbent (mg g^{-1}) at equilibrium and time t, respectively, and k_1 is the rate constant of adsorption (min^{-1}). When ln ($q_e - q_t$) was plotted against time, a straight line should be obtained with a slope of $-k_1$, if the first-order kinetics is valid.

The pseudo-second-order model (Akcay 2004, Ho and McKay 1998) has the following form:

$$t/q_t = t/q_e + 1/\left(k_2 q_e^2\right) \quad (2)$$

Where q_e and q_t represent the amount of Co(II) adsorbed (mg g^{-1}) at equilibrium and at any time, k_2 in the rate constant of the pseudo-second-order equation (g mg^{-1} min^{-1}). A plot of t/q versus time (t) would yield a line with a slope of $1/q_e$ and an intercept of $1/(k_2 q_e^2)$, if the second-order model is a suitable expression.

The plot between ln ($q_e - q_t$) versus time t shows the pseudo-first-order model and the plot of t/q versus time t shows the pseudo-second-order model (Figs. 7 and 8).

The kinetic model with a higher correlation coefficient r^2 was selected as the most suitable one.

It was found that application of pseudo-second-order kinetics provides better correlation coefficient of experimental data than the pseudo-first-order model for the Co(II) onto composite sorbent. The good correlation coefficients were obtained by fitting the experimental data to Eq. (2), indicating that the adsorption process on Fe_3O_4/bentonite is pseudo-second order. In previous papers, the pseudo-second-order kinetic model was found to be appropriate for describing kinetics of metal sorption (Feng et al. 2010). The values of rate constant were calculated from the slope of the Figs. 7 and 8 are represented at Table 2.

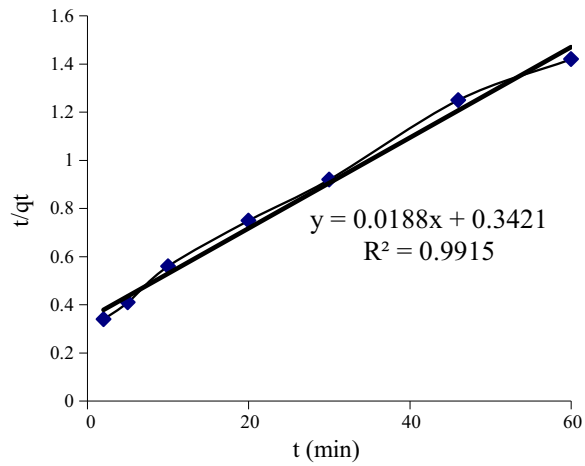

Fig. 8 Pseudo-second-order kinetics for adsorption of Co(II) on Fe_3O_4/bentonite composite Co(II) solution, initial concentration 800 mg L^{-1}, pH 8, and 0.1 g adsorbent)

Table 2 Kinetics parameters for the removal of Co(II) by Fe_3O_4/bentonite

First order		Second order	
R^2	K_1 (min^{-1})	R^2	K_2 (g mg^{-1} min^{-1})
0.845	0.0234	0.991	1.03×10^{-3}

3.6 Adsorption Isotherm

Adsorption capacity and adsorption behavior of Co(II) on bentonite, Fe_3O_4, and Fe_3O_4/bentonite nanocomposite can be illustrated by adsorption isotherm. Data from the adsorption isotherms were modeled using the Langmuir and Freundlich isotherm models with the resulting isotherm constants presented in Table 3.

The Langmuir isotherm theory is based on the assumption of adsorption on a homogenous surface. The Langmuir equation can be written in the following form:

$$q_e = q_m K_L C_e/(1 + K_L C_e) \quad (3)$$

The linearized form of Langmuir can be written as follows (Fig. 9):

$$C_e/q_e = 1/q_m K_L + C_e/q_m \quad (4)$$

Where q_e is the solid-phase equilibrium concentration (mg g^{-1}); C_e is the liquid equilibrium concentration of Co(II) in solution (mg L^{-1}); K_L is the equilibrium constant related to the affinity of binding sites (L mg^{-1}); and q_m is the maximum amount of the Co(II) per unit weight of adsorbent for complete monolayer coverage.

The Freundlich isotherm describes adsorption where the adsorbent has a heterogeneous surface with adsorption sites that have different energies of adsorption. The energy of adsorption varies as a function of the surface coverage (q_e) and is represented by Freundlich constant K_F (L g^{-1}) in Eq. 5.

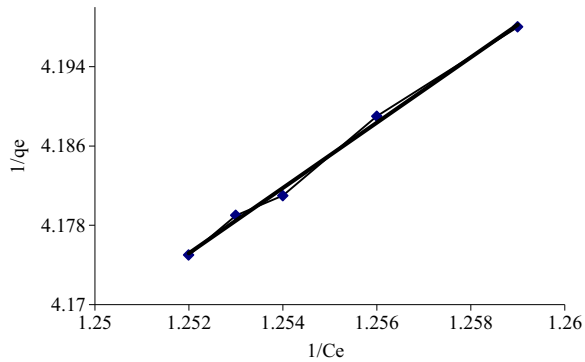

Fig. 9 Langmuir plot for Co(II) on the Fe_3O_4/bentonite composite (50 mL Co(II) solution, initial concentration 800 mg L^{-1}, pH 8, and 0.1 g adsorbent)

$$q_e = K_F C_e^n \quad (5)$$

Where K_F is roughly an indicator of the adsorption capacity and n is the heterogeneity factor which has a lower value for more heterogeneous surfaces.

In most references, Freundlich adsorption Eq. (5) may also be expressed as Eq. (6) (Fig. 10):

$$\ln q_e = \ln K_F + 1/n \ln C_e \quad (6)$$

All the correlation coefficients, R^2 value, and the constants obtained for the models from Table 2 show that the Langmuir isotherm is the suitable equation to describe the adsorption equilibrium of Co(II) on the Fe_3O_4/bentonite composite (Liu et al. 2011).

3.7 Thermodynamic Parameters

The effect of temperature is a major influencing factor in the sorption process. In any adsorption process, entropy

Table 3 Langmuir and Freundlich isotherm constant for adsorption of Co(II) onto Fe_3O_4/bentonite composite

Sorbents	Langmuir model			Freundlich model		
	q_m (mg g^{-1})	K_l (L mg^{-1})	R^2	K_F (mg g^{-1})	$1/n$	R^2
Bentonite	9.97	0.014	0.994	0.275	6.2	0.95
Fe_3O_4	15.22	0.022	0.991	0.324	24.5	0.96
Fe_3O_4/bentonite	18.76	0.072	0.996	0.402	8.3	0.98

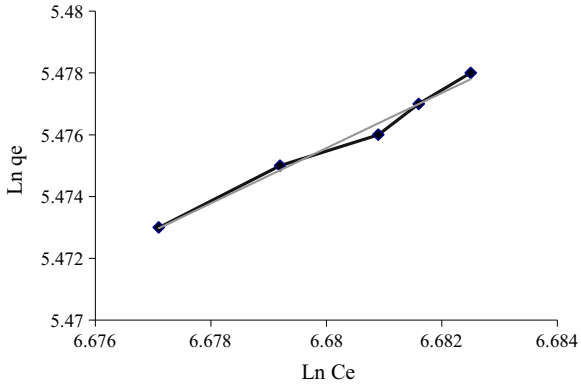

Fig. 10 Freundlich plot for Co(II) on the Fe_3O_4/bentonite composite (50 mL Co(II) solution, initial concentration 800 mg L^{-1}, initial pH 8, and 0.1 g adsorbent)

consideration must be taken into account in order to determine which process will occur spontaneously. Values of thermodynamic parameters are the actual indicators for practical application of a process. The amount of Co(II) adsorbed at equilibrium at different temperatures 15–60 °C has been examined to obtain thermodynamic parameters for the adsorption system. The thermodynamic parameters, change in the standard free energy ($\Delta G°$), enthalpy ($\Delta H°$) and entropy ($\Delta S°$) associated with the adsorption process, and these were determined using the following equations (Dogan et al. 2004):

$$\Delta G^\circ = -RT \ln K_C \tag{7}$$

Where $\Delta G°$ is the standard free energy change, R the universal gas constant (8.314 J mol^{-1} K^{-1}), T the absolute temperature, and K_C the equilibrium

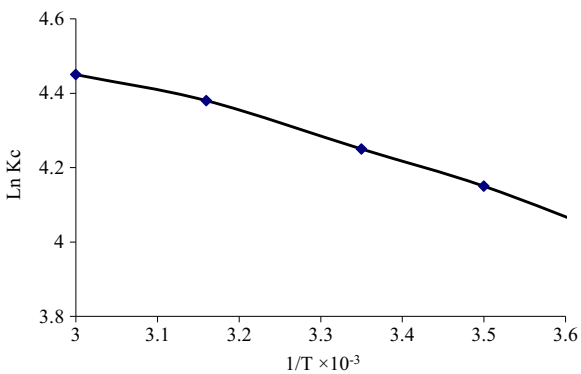

Fig. 11 plot of ln K_c verses $1/T$ for estimation of thermodynamic parameter (50 mL Co(II) solution, initial concentration 800 mg L^{-1}, pH 8, and 0.1 g adsorbent)

Table 4 Thermodynamic parameters of Co(II) onto Fe_3O_4/bentonite composite (0.1 g sorbent, 50 mL Co(II) 800 mg L^{-1}, pH 10)

Sample	T (K)	K_c	$\Delta G°$ (kJ mol^{-1})	$\Delta H°$ (J mol^{-1})	$\Delta S°$ (J mol^{-1} k^{-1})
Co(II)	288	53.23	−9/02	5.95	−55.09
	293	62.60	−9/89		
	298	72.61	−10/60		
	313	78.26	−11/34		
	333	84.87	−12/29		

constant. The apparent equilibrium constant of the sorption, K_C, is obtained from:

$$K_C = C_A / C_S \tag{8}$$

Where K_C is the equilibrium constant, C_A is the amount of dye adsorbed on the adsorbent of solution at equilibrium (mg L^{-1}), and C_S is the equilibrium concentration of dye in the solution (mg L^{-1}). K_C values were calculated at different temperatures to allow the determination of the thermodynamic K_C (Iqbal and Ashiq 2007; Bulut and Aydin 2006). The free energy changes are also calculated by using the following equations:

$$ln\, K_C = -\Delta G^\circ / RT = -\Delta H^\circ / RT + \Delta S^\circ / R \tag{9}$$

$\Delta H°$ and $\Delta S°$ were calculated from the slope and intercept of Van't Hoff plots of ln K_C versus $1/T$ (Fig. 11). The results are given in Table 4.

The negative $\Delta G°$ values indicated thermodynamically feasible and spontaneous nature of the adsorption of Co(II). The decrease in negative $\Delta G°$ values together with an increase in temperatures shows an increase in feasibility of sorption at higher temperatures. The $\Delta H°$ parameter was found to be 5.95×10^{-3} kJ/mol. The positive $\Delta H°$ indicates the endothermic nature of the sorption process. Furthermore, the negative value of $\Delta S°$ reveals the decreased randomness at the soils-solution interface during the fixation of cobalt ion on the active sites of the sorbent (Mahmood et al. 2011; Liu et al. 2011).

4 Conclusion

Nanocrystalline Fe_3O_4 and Fe_3O_4/bentonite composite with spinel structure were successfully synthesized by a

chemical co-precipitation method. The XRD and TEM results illustrated that the nanoparticles have good crystallinity with fine cubic spinel structure. The nanospinels exhibit regular morphology with homogeneous particle size distribution. The FTIR spectroscopy confirmed the structure of obtained nanoparticles. The Fe_3O_4/bentonite composite acts as a novel low-cost adsorbent material for the removal of Co(II) from aqueous solutions. The amount of Co(II) adsorbed was varying with initial pH, adsorbent dose, and initial concentration of Co(II). The adsorption kinetics of Co(II) was found to follow pseudo-second-order model. The Langmuir and Freundlich adsorption models were used to express the sorption. The Langmuir adsorption isotherm was found to have the best fit to the experimental data. The results of thermodynamics referred the negative value of $\Delta G°$ and spontaneously process.

References

Abollino, O., Aceto, M., Malandrino, M., Sarzanini, C., & Mentasti, E. (2003). Adsorption of heavy metals on Na-montmorillonite. Effect of pH and organic substances. *Water Research, 37*, 1619–1627.

Akcay, M. (2004). Characterization and determination of the thermodynamic and kinetic properties of p-CP adsorption onto organophilic bentonite from aqueous solutions. *Journal of Colloid and Interface Science, 280*, 299–304.

Bulut, Y., & Aydin, H. (2006). A kinetic and thermodynamics study of methylene blue adsorption on wheat shells. *Desalination, 194*, 259–267.

Chang, Y. C., & Chen, D. H. (2005). Preparation and adsorption properties of mono disperse chitosan-bound Fe_3O_4 magnetic nanoparticles for removal of Cu (II) ions. *Journal of Colloid Interface Science, 283*, 446–461.

Dogan, M., Alkan, M. A., & Tŭrkyilmaz, Y. (2004). Kinetics and mechanism of removal of methylene blue by adsorption onto perlite. *Journal of Hazardous Materials, B109*, 141–148.

Eren, E., & Afsin, B. (2008). An investigation of Cu (II) adsorption by raw and acid-activated bentonite: a combined potentiometric, thermodynamic, XRD, IR, DTA study. *Journal of Hazardous Materials, 151*, 682–691.

Feng, Y., Gong, J. L., Zeng, G. M., Niu, Q. Y., Zhang, H. Y., Niu, C. G., Deng, J. H., & Yan, M. (2010). Adsorption of Cd (II) and Zn (II) from aqueous solutions using magnetic hydroxyapatite nanoparticles as adsorbents. *Chemical Engineering Journal, 162*, 487–494.

Galamboš, M., Rosskopfová, O., Kufčáková, J., & Rajec, P. (2011). Utilization of Slovak bentonites in deposition of high-level radioactive waste and spent nuclear fuel. *288*(3), 765–777.

Galambošm, M., Suchánek, P., & Rosskopfová, M. (2012). Sorption of anthropogenic radionuclides on natural and synthetic inorganic sorbents. *Journal of Radioanalytical and Nuclear Chemistry, 293*(2), 613–633.

Gallions, G. P., & Vaclavikova, A. (2008). Removal of Cr (VI) from water stream. *Environmental Chemistry Letters, 6*, 235–240.

Gupta, V. K., Suhas, S., & Mohan, D. (2003). Equilibrium uptake and sorption dynamics for the removal of a basic dye (basic red) using low-cost adsorbents. *Journal of Colloid Interface Science, 265*, 257–264.

Hashemian, S. (2007). Study of adsorption of acid dye from aqueous solutions using bentonite. *Main Group Chemistry, 6*, 97–107.

Hashemian, S. (2010). $MnFe_2O_4$/bentonite nano composite as a novel magnetic material for adsorption of acid red 138. *African Journal of Biotechnology, 9*(50), 8667–8671.

Hashemian, S. (2011). Removal of Acid Red 151 from water by adsorption onto nano-composite $MnFe_2O_4$/kaolin. *Main Group Chemistry, 10*, 105–114.

Hashemian, S., & Foroghimoqhadam, A. (2014). Effect of copper doping on CoTiO3 Ilmenite type nano particles for removal of congo red from aqueous solution. *Chemical Engineering Journal, 235*, 299–306.

Ho, Y. S., & McKay, G. (1998). Pseudo-second order model for sorption process. *Chemical Engineering Journal, 70*, 115–124.

Iqbal, M. J., & Ashiq, M. N. (2007). Asorption of dyes from aqueous solutions on activated charcoal. *Journal of Hazardous Materials B, 139*, 57–66.

Kalyani, S., Krishnaiah, A., & Boddu, V. M. (2007). Adsorption of divalent cobalt from aqueous solution onto chitosan-coated perlite beads as biosorbent. *Separ Science Technology, 42*(12), 2768–2786.

Kara, M., Yuzer, H., Sabah, E., & CelikM, S. (2003). Adsorption of cobalt from aqueous solutions onto sepiolite. *Water Research, 37*(1), 224–232.

Khenifi, A., Bouberka, F., Kameche, M., Derriche, Z. (2007). Adsorption study of an industrial dye by organic clay. *13*(2), 149–158.

Kobya, M., Demirbas, E., Senturk, E., & Ince, M. (2005). Adsorption of heavy metal ions from aqueous solutions by activated carbon prepared from apricot stone. *Bioresearch Technology, 96*(13), 1518–1521.

Liu, Y., Liu, Z., Dai, J., Gao, J., Xie, J., & Yan, Y. (2011). Selective adsorption of Co(II) by mesoporous silica SBA-15-supported surface ion imprinted polymer: kinetics, isotherms, and thermodynamics studies. *Chinese Journal of Chemistry, 29*(3), 387–397.

Mahmood, T., Saddique, M. T., Naeem, A., Mustafa, S., Zeb, N., Shah, K. H., & Waseem, M. (2011). Kinetic and thermodynamic study of Cd(II), Co(II) and Zn(II) adsorption from aqueous solution by NiO. *Chemical Engineering Journal, 171*(3), 935–940.

Meng, J., Yan, G., Yan, L., & Wang, X. (2005). Synthesis and characterization of magnetic nanometer pigment Fe_3O_4. *Dyes and Pigments, 66*, 109–113.

Mockovčiaková, A., Orolínová, Z., & Skvarla, J. (2010). Enhancement of the bentonite sorption properties. *Journal of Hazardous Materials, 180*, 274–281.

Naiya, T. K., Bhattacharya, A. K., & Kumar, S. (2009). Adsorption of Cd(II) and Pb(II) from aqueous solutions on activated alumina. *Journal of Colloid Interface Science, 333*(1), 14–26.

Namasivayam, C., & Sureshkumar, M. V. (2008). Removal of Cr (VI) from waste and wastewater using surfactant modified coconut coir pith as a biosorbent. *Bioresearch Tecnology, 99*(7), 2218–2225.

Oliveira, L. C. A., Rachel, V. R. A. R., Fabris, J. D., Sapag, K., Vijayendra, K. G., & Lago, R. M. (2003). Clay–iron oxide magnetic composites for the adsorption of contaminants in water. *Applied Clay Science, 22*, 169–177.

Orolínová, Z., Mockovčiaková, A., & Škvarla, J. (2010). Sorption of cadmium (II) from aqueous solution by magnetic clay composite. *Desalination and Water Treatment, 24*, 284–292.

Özer, D., Dursum, G., & Özer, A. (2007). Methylene blue adsorption from aqueous solutions by dehydrated peanut hull. *Journal of Hazardous Materials, 144*, 171–179.

Ramakrishna, K. R., & Viraraghavan, T. (1997). Dye removal using low cost adsorbents. *Water Science and Technology, 36*(2–3), 189–196.

Rengaraj, S., Yeon, K. H., Kang, S. Y. K., Lee, J. U., Kim, K. W., & Moon, S. H. (2002). Studies on adsorptive removal of Co(II), Cr(III) and Ni(II) by IRN77 cation-exchange resin. *Journal of Hazardous Materials, B92*, 185–198.

Smiciklas, A., Dimovic, S., & Plecas, I. (2007). Removal of Cs^{1+}, Sr^{2+} and Co^{2+} from aqueous solutions by adsorption on natural clinoptilolite. *Applied Clay Science, 35*(1–2), 139–144.

Tamez Uddin, M., Akhtarul Islam, M., Mahmud, S., & Rukanuzzaman, M. (2009). Adsorptive removal of methylene blue by tea waste. *Journal of Hazardous Materials, 164*, 53–60.

Üzüm, C., Shahwan, T., Eroğlu, A. E., Hallam, K. R., Scott, T. B., & Lieberwirth, I. (2009). Synthesis and characterization of kaolinite-supported zero-valent iron nanoparticles and their application for the removal of aqueous Cu^{2+} and Co^{2+} ions. *Applied Clay Science, 43*, 172–181.

Vereš, J., Z. Orolĺnová, Z., Mockovčiaková. A., Jakabský, S., Bakalár, T. (2010). Removal of nickel by natural and magnetically modified bentonite. water treatment technologies for the removal of high-toxicity pollutants. (2010) 289–294.

Villalba, J. C., Constantino, V. R. L., & Anaissi, F. J. (2010). Iron oxyhydroxide nanostructured in montmorillonite clays: preparation and characterization. *Journal of Colloid Interface Science, 349*, 49–55.

Wu, R., & Qu, J. (2005). Removal of water-soluble azo dye by the magnetic material $MnFe_2O_4$. *Journal of Chemical Technology and Biotechnology, 27*, 20–27.

Wu, R., Qu, J., He, H., & YU, Y. (2004). Removal of azo-dye acid red B (ARB) by adsorption and catalytic combustion using magnetic $CuFe_2O_4$ powder. *Applied Catalysis B: Environment, 48*, 49–56.

Wu, R., Qu, J., & Chen, Y. (2005). Magnetic powder MnO-Fe_2O_3 composite—a novel material of azo-dye from water. *Water Research, 39*, 630–638.

Yang, N. (2008). Anatase TiO_2 nanolayer coating on cobalt ferrite nanoparticles for magnetic photo catalyst. *Materials Letters, 62*, 645–647.

Yavuz, O., Altunkaynak, Y., & Guzel, F. (2003). Removal of copper, nickel, cobalt and manganese from aqueous solution by kaolinite. *Water Research, 37*(4), 948–952.

Zhang, G., Qu, J., Liu, H., Cooper, A. T., & Wu, R. (2007). $CuFe_2O_4$/activated carbon composite: a novel magnetic adsorbent for the removal of acid orange II and catalytic regeneration. *Chemosphere, 68*(6), 1058–1066.